

# Revisiting Low-Frequency Susceptibility Data in Superconducting Materials

Jacob Szeftel<sup>1, \*</sup>, Michel Abou Ghantous<sup>2</sup>, and Nicolas Sandeau<sup>3</sup>

**Abstract**—Old susceptibility data, measured in superconducting materials at low-frequency, are shown to be accounted for consistently within the framework of a recently published [1] analysis of the skin effect. Their main merit is to emphasize the significance of the skin-depth measurements, performed *just beneath* the critical temperature  $T_c$ , in order to disprove an assumption, which thwarted any understanding of the skin-depth data, achieved so far by conventional high-frequency methods, so that those data might, from now on, give access to the temperature dependence of the concentration of superconducting electrons.

## 1. INTRODUCTION

Very low-frequency ( $\omega < 40$  Hz) measurements [2, 3], carried out in superconducting materials, exhibited the absorption part of complex susceptibility rising to a maximum  $\chi''(T_M)$ , located close to  $T_c$  (see Fig. 1), which the authors then ascribed to the vortex lattice, typical of superconductors of type II. However, as this feature was subsequently observed also in materials of type I, an alternative explanation [4], relying heavily on the BCS gap [5, 6], was proposed. Anyhow, both interpretations [2–4] turn out to be at best qualitative and partial, since the maximum of the absorption has also been observed in high- $T_c$  compounds [7, 8], all of which are gapless superconductors of type II, undergoing a magnetic field  $H < H_{c1}$ , which warrants the absence of vortex. Noteworthy is that those susceptibility measurements [7, 8] were interpreted solely with help of the skin effect theory, valid for normal metals [9, 10]. Likewise, we shall confirm below this latter explanation, by showing *quantitatively* that the low frequency behavior of the susceptibility can indeed be fully understood as a straightforward by-product of the macroscopic skin effect [1], valid for superconductors of both kinds as well, regardless of whether they display a BCS gap or not.

In every conductor, the real part of the dielectric constant being negative for  $\omega < \omega_p$ , where  $\omega_p \approx 10^{16}$  Hz stands for the plasma frequency, causes the electromagnetic field to remain confined within a thin layer of frequency dependent thickness  $\delta(\omega)$ , called the skin depth [9, 10], and located at the outer edge of the conductor. The first measurement of  $\delta$  in superconductors was done, at a *single* frequency  $\omega \approx 10$  GHz, by Pippard [11], who *assumed, without any proof*,  $\omega$ -independent  $\delta$ . The current state of affairs, regarding measurements of the skin-depth in superconductors, including both low- and high- $T_c$  materials, is muddled. On one hand, some authors [12, 13], in the wake of Pippard's work, tend to *assume*  $\delta(\omega) = \lambda_L, \forall \omega$ . London's length  $\lambda_L$  is defined [14] as  $\lambda_L = \sqrt{\frac{m}{\mu_0 c_s e^2}}$ , with  $\mu_0, e, m, c_s$  standing for the magnetic permeability of vacuum, the charge, effective mass and concentration of superconducting electrons, respectively. Besides, it has long been believed [14] that  $\lambda_L = \lambda_M$ , with  $\lambda_M$  being the penetration depth of a *static* magnetic field into a superconductor, characterizing the

---

Received 8 October 2018, Accepted 3 December 2018, Scheduled 21 December 2018

\* Corresponding author: Jacob Szeftel (jszeftel@lpqm.ens-cachan.fr).

<sup>1</sup> ENS Cachan, LPQM, 61 avenue du Président Wilson, Cachan 94230, France. <sup>2</sup> American University of Technology, AUT Halat, Highway, Lebanon. <sup>3</sup> Aix Marseille Univ, CNRS, Centrale Marseille, Institut Fresnel, Marseille F-13013, France.

Meissner effect [15]. On the other hand, low-frequency susceptibility data have been convincingly explained [7,8] within the framework of the skin effect theory [9,10], which predicts the well-known behavior  $\delta(\omega) \propto 1/\sqrt{\omega}$ , observed in all normal metals. Finally both conjectures  $\delta(\omega) = \lambda_L, \forall \omega$  and  $\lambda_L = \lambda_M$ , which have been questioned recently [1,15], will be rebutted below, by taking advantage of the low-frequency susceptibility data [2,3,7,8].

This analysis will be led within the two-fluid model [6,16], for which the conduction electrons make up a homogeneous mixture, in thermal equilibrium at temperature  $T$ , of normal and superconducting electrons of respective concentrations  $c_n(T), c_s(T)$ , constrained for  $T \leq T_c$ , by  $c_n(T) + c_s(T) = c_0$ , with  $c_0$  being the total concentration of conduction electrons. Consequently, as  $T$  decreases from  $T_c$  down to  $T = 0$ ,  $c_n(T)$  decreases from  $c_n(T_c) = c_0$ , while  $c_s(T)$  increases from  $c_s(T_c) = 0$ .

The outline is as follows: the electrodynamics of the skin effect, developed elsewhere [1], will be recalled in Section 2; this will then be used to reckon the complex susceptibility  $\chi'(\delta) + i\chi''(\delta)$  in Section 3; in Section 4, the calculated  $\chi''(\delta)$  and the experimental data  $\chi''(T)$ , available in Fig. 1, will be taken advantage of to achieve  $\delta(T < T_c)$ , but foremost, to rebut the surmise  $\delta(\omega) = \lambda_L, \forall \omega$ , widely used for the interpretation of skin-depth data, obtained [12,13] at high-frequency. The conclusions are given in Section 5.

Before proceeding below with the discussion of the  $\chi''(T \leq T_c)$  data, it is worth noticing, in Fig. 1, the dispersion  $\chi'(T)$  swinging abruptly at  $T_c$  from  $\chi'(T > T_c) < 0$  in the normal phase to  $\chi'(T < T_c) > 0$  in the superconducting one. This property, which has been ascribed [15] to the normal and superconducting states, being paramagnetic and diamagnetic, respectively, has furthermore been argued to be responsible for the Meissner effect, observed in a field-cooled sample. Therefore, the gratifying agreement with the experimental evidence, displayed in Fig. 1, should contribute to ascertaining the validity of our conclusion [15]  $\lambda_L \ll \lambda_M$ , which opposes the mainstream claim [14]  $\lambda_L = \lambda_M$ .

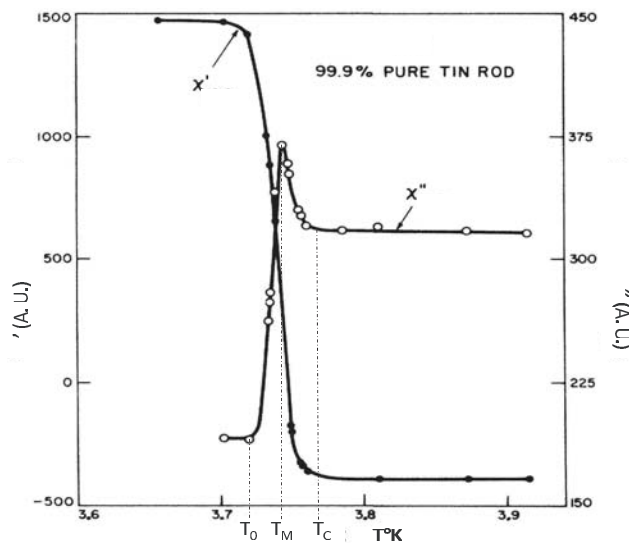


**Figure 1.** Plot of the complex susceptibility  $\chi'(T) + i\chi''(T)$  ( $\chi', \chi''$  stand respectively for dispersion and absorption), as measured by Maxwell and Strongin [2] in superconducting tin ( $T_c = 3.76$  K) at 18.2 Hz;  $T_M = 3.74$  K is the temperature associated with the maximum value of  $\chi''$ ;  $T_0 = 3.72$  K is the temperature, below which  $\chi''(T \leq T_0)$  remains constant.

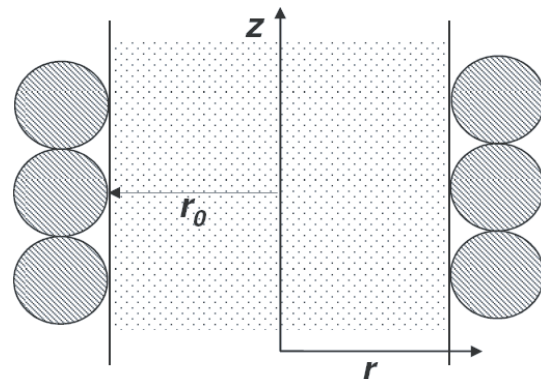


**Figure 2.** Cross-section of the superconducting sample (dotted) and the coil (hatched);  $E_\theta, j_\theta$  are both normal to the unit vectors along the  $r$  and  $z$  coordinates, whereas  $B_z, H_z$  are parallel to the unit vector along the  $z$  axis.

## 2. SKIN EFFECT

A paramount conclusion of the study of the skin effect [1] is that there is no difference in that respect between normal and superconducting metals. Consequently, within the two-fluid model, all of the electro-dynamical properties of any superconducting material depend only on its conductivity [17]  $\sigma = \frac{c_0 e^2 \tau}{m}$ , with  $\tau$  being the decay time of the current, due to its friction on the atomic lattice.  $\sigma$  is calculated as some average [1] over the normal and superconducting conductivities  $\sigma_n = \frac{c_n e^2 \tau_n}{m}$ ,  $\sigma_s = \frac{c_s e^2 \tau_s}{m}$ , respectively, to be discussed later in Section 4. Besides, the superconducting decay time  $\tau_s$  is *finite*, as recalled by Schrieffer [6] (see [6] p. 4, 2nd paragraph, lines 9,10: *at finite temperature, there is a finite ac resistivity for all frequencies > 0*). Moreover, this property of  $\tau_s$  being finite will be demonstrated in Section 4.

Consider as in Fig. 2 a superconducting material of cylindrical shape, characterized by its symmetry axis  $z$  and radius  $r_0$  in a cylindrical frame with coordinates  $(r, \theta, z)$ , which has been inserted into a coil of same radius  $r_0$ . An oscillating current  $I(t) = I_0 e^{i\omega t}$ , with  $t$  referring to time, is fed into the coil. Then  $I(t)$  induces [1], throughout the sample, i.e., for  $r \leq r_0$ , a magnetic field  $H(t, r) = H_z(r) e^{i\omega t}$ , parallel to the  $z$  axis, and an electric field  $E(t, r) = E_\theta(r) e^{i\omega t}$ , normal to the unit vectors along the  $r$  and  $z$  coordinates.  $E$  in turn induces, inside the sample, a current  $j(t, r) = j_\theta(r) e^{i\omega t}$ , parallel to  $E_\theta$ , as given by Newton's law [1]

$$\frac{dj}{dt} = \frac{\sigma}{\tau} E - \frac{j}{\tau}, \quad (1)$$

where  $\frac{\sigma}{\tau} E$  and  $-\frac{j}{\tau}$  are respectively proportional to the driving force accelerating the conduction electrons and a friction term, responsible for Ohm's law [1].

The electric field  $E$  and the magnetic induction  $B(t, r) = \mu_0 H(t, r) = B_z(r) e^{i\omega t}$ , parallel to the  $z$  axis (the relationship between  $H, B$  reads in general  $B = \mu_0(1 + \chi)H$ , which reduces here to  $B = \mu_0 H$ , because of  $|\chi| \ll 1$ , as proved elsewhere [15]) are related [1] through the Faraday-Maxwell equation as

$$-\frac{\partial B}{\partial t} = \frac{E}{r} + \frac{\partial E}{\partial r}. \quad (2)$$

Finally, the magnetic field  $H$  and current  $j$  are related [1] through the Ampère-Maxwell equation as

$$-\frac{\partial H}{\partial r} = 2j + \epsilon_0 \frac{\partial E}{\partial t}, \quad (3)$$

with  $\epsilon_0$  referring to the electric permittivity of vacuum.

Replacing  $E(t, r), j(t, r), B(t, r), H(t, r)$  in Eqs. (1), (2), (3), by their time-Fourier transforms  $E_\theta(\omega, r), j_\theta(\omega, r), B_z(\omega, r), H_z(\omega, r)$  yields [1]

$$\begin{aligned} E_\theta(\omega, r) &= \frac{1 + i\omega\tau}{\sigma} j_\theta(\omega, r) \\ i\omega B_z(\omega, r) &= - \left( \frac{E_\theta(\omega, r)}{r} + \frac{\partial E_\theta(\omega, r)}{\partial r} \right) \\ \frac{\partial B_z(\omega, r)}{\partial r} &= -\mu_0 (2j_\theta(\omega, r) + i\omega\epsilon_0 E_\theta(\omega, r)) \end{aligned} \quad (4)$$

Eliminating  $E_\theta(\omega, r), j_\theta(\omega, r)$  from Eq. (4) gives [1] finally

$$\frac{\partial^2 B_z(\omega, r)}{\partial r^2} = \frac{B_z(\omega, r)}{\delta^2(\omega)} - \frac{\partial B_z(\omega, r)}{r \partial r}, \quad \delta(\omega) = \frac{\lambda_L}{\sqrt{1 + i\omega\tau - \frac{\omega^2}{\omega_p^2}}}, \quad (5)$$

with the plasma frequency defined [9, 10, 16] as  $\omega_p = \sqrt{\frac{c_0 e^2}{\epsilon_0 m}}$ . Eq. (5) yields [1] indeed both the usual expression  $|\delta| = \frac{1}{\sqrt{2\mu_0 \sigma \omega}}$ , valid in the low frequency limit  $\omega\tau \ll 1$ , and its lower bound  $\delta = \frac{\lambda_L}{\sqrt{2}}$ , reached at high frequency such that  $\omega\tau \gg 1$ .

### 3. LOW-FREQUENCY SUSCEPTIBILITY

Due to  $\delta = \frac{1}{\sqrt{2i\mu_0\sigma\omega}}$ , if  $\omega\tau \ll 1$ , as inferred from Eq. (5), the complex induction reads  $B_z(u) = B_r(u) + iB_i(u)$ , with  $u = \frac{r}{|\delta|}$ , so that Eq. (5) can be recast into

$$\frac{\partial^2 B_r}{\partial u^2} = -B_i - \frac{\partial B_r}{u\partial u}, \quad \frac{\partial^2 B_i}{\partial u^2} = B_r - \frac{\partial B_i}{u\partial u}. \quad (6)$$

The system of linear differential equations in Eq. (6) has been integrated over  $u \in \left[0, \frac{r_0}{|\delta|}\right]$  with the following boundary conditions

$$\frac{dB_r}{du}(0) = \frac{dB_i}{du}(0) = 0, \quad B_r\left(\frac{r_0}{|\delta|}\right) = B_r(I_0), \quad B_i\left(\frac{r_0}{|\delta|}\right) = B_i(I_0).$$

The complex induction  $B(I_0) = B_r(I_0) + iB_i(I_0)$ , induced at  $r_0$  by the current  $I$  flowing through the coil, has been calculated elsewhere [1] to read  $\frac{B(I_0)}{I_0} \propto 2 - i\epsilon_0\rho_c\omega$ , with  $\rho_c$  being the resistivity of the coil.

The complex self-inductance  $L$  of the system, made up of the coil and the superconducting sample, reads as  $L \propto \chi' + i\chi''$ . Due to the very definition of  $L = \frac{2\pi}{I_0} \int_0^{r_0} B_z(r)rdr$ , the susceptibility reads finally

$$\chi' \propto |\delta|^2 \int_0^{\frac{r_0}{|\delta|}} B_r(u)udu, \quad \chi'' \propto |\delta|^2 \int_0^{\frac{r_0}{|\delta|}} B_i(u)udu.$$

$\chi'\left(\frac{r_0}{|\delta|}\right)$ ,  $\chi''\left(\frac{r_0}{|\delta|}\right)$  have been plotted in Fig. 3(a). The characteristic features, mentioned elsewhere [2, 3, 7, 8], can be seen conspicuously, namely  $\chi'\left(\frac{r_0}{|\delta|}\right)$  decreases monotonically, whereas  $\chi''\left(\frac{r_0}{|\delta|}\right)$  goes through a maximum  $\chi^M$  at  $\frac{r_0}{|\delta|} = 2.53$ . The maximum was reported [2, 3] previously to show up rather at  $\frac{r_0}{|\delta|} \approx 1.8$ . This discrepancy is to be ascribed to a different definition of the susceptibility, chosen there [2–4], which nevertheless does not correspond, unlike the definition used here, to what is actually measured in the experimental procedure, i.e., the complex impedance of the circuit, comprising the coil and the sample. The data in Fig. 3(a) are independent from  $\omega$  because  $\omega$  shows up only in the

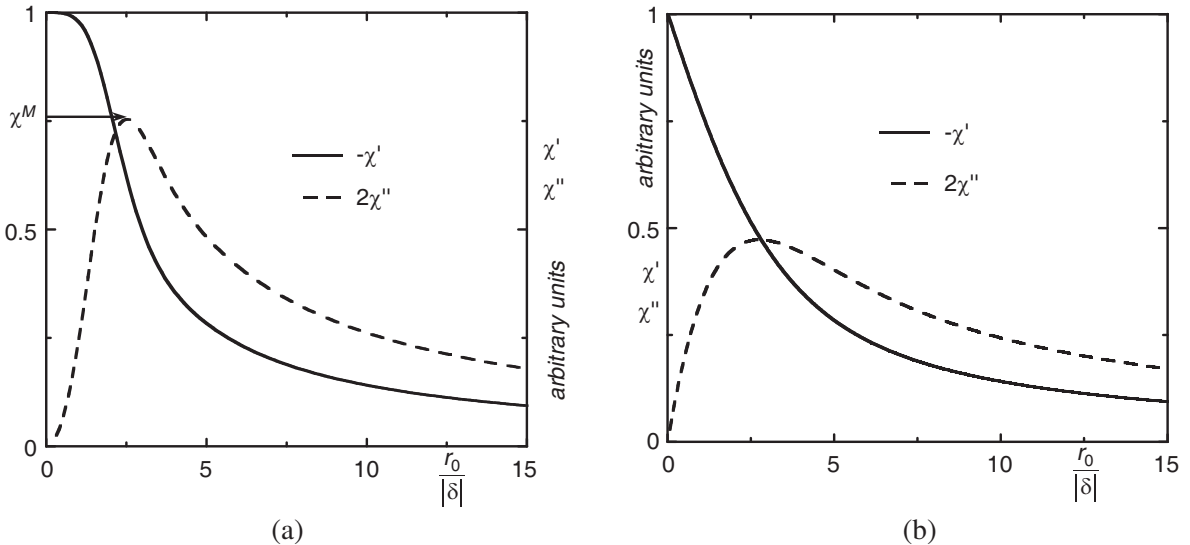


**Figure 3.** Plots of the complex susceptibility  $\chi' + i\chi''$  versus  $\frac{r_0}{|\delta|}$ , calculated with help of the solution of Eq. (5) and Eq. (7), in Fig. 3(a) and Fig. 3(b), respectively.

expression of  $B_i(I_0)$ , which turns out to be negligible ( $\left| \frac{B_i(I_0)}{B_r(I_0)} \right| \approx 10^{-18}$  for  $\omega = 100$  Hz). However they do *depend* on the sample *shape*, as illustrated by reckoning the susceptibility for the semi-infinite slab considered by London [14]. In this latter case, Eq. (5) should be replaced by

$$\frac{\partial^2 B_z}{\partial r^2} = \frac{B_z}{\delta^2} \Rightarrow B_z(u) \propto 2e^{\frac{1+i}{\sqrt{2}}\left(u - \frac{r_0}{|\delta|}\right)}, \quad (7)$$

which entails that  $\chi', \chi''$  read now

$$\chi' \propto \frac{|\delta|}{\sqrt{2}r_0} - \frac{e^{-\frac{r_0}{\sqrt{2}|\delta|} \sin\left(\frac{r_0}{\sqrt{2}|\delta|}\right)}}{\left(\frac{r_0}{\sqrt{2}|\delta|}\right)^2}, \quad \chi'' \propto -\frac{|\delta|}{\sqrt{2}r_0} + \frac{1 - e^{-\frac{r_0}{\sqrt{2}|\delta|} \cos\left(\frac{r_0}{\sqrt{2}|\delta|}\right)}}{\left(\frac{r_0}{\sqrt{2}|\delta|}\right)^2}.$$

The corresponding  $\chi' \left(\frac{r_0}{|\delta|}\right)$ ,  $\chi'' \left(\frac{r_0}{|\delta|}\right)$  data are depicted in Fig. 3(b). Note that the maximum value of  $\chi''$  shifts from  $\frac{r_0}{|\delta|} = 2.53$  in Fig. 3(a) up to  $\frac{r_0}{|\delta|} = 2.77$  in Fig. 3(b). Likewise the ratios  $\chi'/\chi''$  differ from each other for any  $r_0/|\delta|$  in both figures. Those differences stem from the respective solutions  $B_z(u)$  of Eqs. (5), (7) deviating from each other in the relevant domain, i.e., for  $u \approx 1$ , even though they are practically identical for  $u \gg 1$ , because the solution of Eq. (5) is a Bessel function, having the property  $B_z(r) \approx e^{r/\delta(\omega)}$  if  $r \gg |\delta(\omega)|$ .

#### 4. EXPERIMENTAL DISCUSSION

We shall now take advantage of both  $\chi''(T)$  data, taken from Fig. 1, and  $\chi''(\delta)$  ones, pictured in Fig. 3(a), to chart  $\delta(T \leq T_c)$ . The one to one correspondence between  $\chi''(T)$ ,  $\chi''(\delta)$  is then expressed as

$$\frac{\chi''(T > T_M) - \chi''(T_M)}{\chi''(T_c) - \chi''(T_M)} = \frac{\chi''(\delta(T)) - \chi^M}{\chi''(\delta(T_c)) - \chi^M}, \quad \frac{\chi''(T < T_M) - \chi''(T_M)}{\chi''(T_0) - \chi''(T_M)} = \frac{\chi''(\delta(T)) - \chi^M}{\chi''(\delta(T_0)) - \chi^M}.$$

$T_M, T_0$  are defined in the caption of Fig. 1, and  $\chi^M$  refers to the maximum value of  $\chi''(\delta)$  (see Fig. 3(a)). As the values of  $\delta(T_c), \delta(T_0)$  are unknown, we have assumed arbitrarily  $\frac{r_0}{|\delta(T_c)|} = 0.5$ ,  $\frac{r_0}{|\delta(T_0)|} = 41$ , in order to proceed with the detailed discussion of an illustrative example. Finally the resulting  $|\delta(T \leq T_c)|$  curve has been plotted in Fig. 4. Its prominent feature is the large variation of  $|\delta|$ , and thence of  $\sigma$ ,

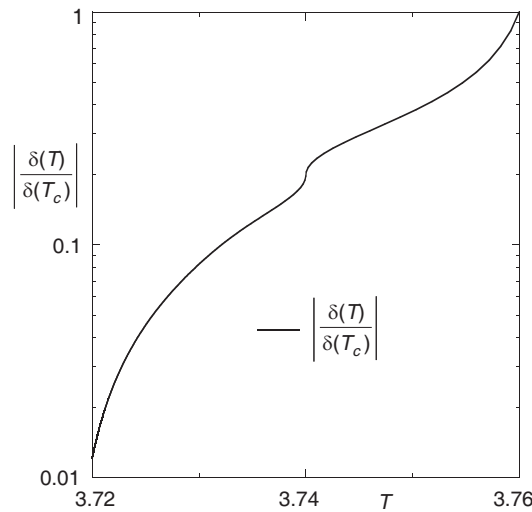


**Figure 4.** Semilogarithmic plot of  $|\delta(T \in [T_0, T_c])|$  with  $T_0 = 3.72$  K and  $T_c = 3.76$  K; the discontinuity of  $\frac{d|\delta|}{dT}$  at  $T_M = 3.74$  K, which reflects that of  $\frac{d\chi''}{dT}(T_M)$  in Fig. 1, is a spurious effect, caused by the experimental difficulty [2] in resolving the narrow temperature range  $[T_0, T_c]$ .

over a narrow temperature range  $T_c - T_0 = 0.04$  K, resulting from the steep decrease of  $c_s$  down to 0 for  $T \rightarrow T_c^-$ , as shown below.

In the two-fluid model,  $\sigma$  reads [1], at low frequency such that  $\omega\tau_s \ll 1$ , as

$$\sigma(T) = \sigma_n + \sigma_s = \frac{e^2}{m} ((c_0 - c_s(T))\tau_n + c_s(T)\tau_s), \quad (8)$$

because of  $c_n(T \leq T_c) + c_s(T) = c_0$ . Consequently, the average  $\tau$ , showing up in Eq. (1), is defined as  $c_0\tau = (c_0 - c_s)\tau_n + c_s\tau_s$ . At low  $T$ , the current decay is due to scattering by impurities and (or) dislocations, so that  $\tau_n, \tau_s$  are  $T$ -independent. Although the value of  $\tau$  is in general unknown, it could be measured as indicated elsewhere [1]. Then the measurement of  $\delta$  would provide with a rather *unique* access to  $c_s(T)$ . The steep increase of  $|\delta|$  for  $T \rightarrow T_c^-$ , seen in Fig. 4, stems from the rapid decrease of  $c_s(T \rightarrow T_c^-) \rightarrow 0$  with  $\tau_n \ll \tau_s$  [1], consistently with Eq. (8).

Besides, both the observed [3, 7, 8] downward shift of  $T_M \searrow 0$  with growing magnetic field  $H$  or impurity concentration and, conversely, the upward one  $T_M \nearrow T_c$ , resulting from increasing the frequency  $\omega$ , are very well accounted for within the framework of this analysis:

- increasing  $H$  has been shown to cause  $c_s$  (see arXiv: 1704.03729), and thence  $\sigma$  (see Eq. (8)) to decrease. Due to  $|\delta| = \frac{1}{\sqrt{2\mu_0\sigma\omega}}$ , decreasing  $\sigma$  leads in turn to increasing  $|\delta|$ . Because the maximum of  $\chi''(\delta)$  is pinned at  $\frac{r_0}{|\delta|} = 2.53$  (see Fig. 3(a)), the maximum of  $\chi''(T_M = T_i(H = 0))$  will be shifted down to  $T_M = T_f(H \neq 0) < T_i$ , owing to  $c_s(T_f < T_i) > c_s(T_i) \Rightarrow \sigma(T_f) > \sigma(T_i)$ , such that  $|\delta(H = 0, T_i)| = |\delta(H \neq 0, T_f)| \Rightarrow \frac{r_0}{|\delta(H=0, T_i)|} = \frac{r_0}{|\delta(H \neq 0, T_f)|} = 2.53$ . Likewise, as increasing the impurity concentration causes both  $\tau$  and thence  $\sigma$  to decrease, the same rationale implies that the maximum of  $\chi''(T)$  will be pushed towards lower  $T$  too;
- conversely, because of  $|\delta(\omega)| \propto 1/\sqrt{\omega}$ , growing  $\omega$  from  $\omega_i$  up to  $\omega_f > \omega_i$  will shift the temperature  $T_i$  of the maximum of  $\chi''(T_M = T_i(\omega_i))$  up to  $T_f(\omega_f > \omega_i) > T_i$ , so that  $\frac{r_0}{|\delta(\omega_i, T_i)|} = \frac{r_0}{|\delta(\omega_f, T_f)|} = 2.53$ .

For low-frequency measurements of  $\chi''(T)$  to be useful, the prerequisite  $|\delta(\omega, T_c)| > r_0$  must be fulfilled. Such a condition requires, in very pure superconductors ( $\Rightarrow$  large  $\tau$ -value), to operate at unpractical low frequency. This is the real reason why Maxwell and Strongin [2] failed to observe any maximum of  $\chi''(T)$  in very pure  $Sn$ . This drawback and the additional one that the values of  $\delta(\omega, T_c), \delta(\omega, T_0)$  are in general unknown, entail that the measurement of the low-frequency susceptibility could not be regarded as a practical alternative method to conventional high-frequency ones [12, 13], currently used to measure the skin-depth. However, due to a special circumstance to be discussed now, it still turns out to be of great relevance.

At high enough a frequency, such that  $r_0 \gg |\delta(\omega)|$ , it has been shown [1] that  $|\delta| = C(\omega)\chi'(\omega, T)$ , for which  $C(\omega)$  is an unknown experimental coefficient. Therefore, assessing the accurate value of  $\delta(T)$  requires to perform the measurement of  $\chi'(T)$  up to  $T_c$ , because the value of  $\sigma(T_c) = \sigma_n(T_c)$  and thence that of  $|\delta(T_c)| = \frac{1}{\sqrt{2\mu_0\sigma_n(T_c)\omega}}$  are well known. However, an accurate assignment of  $\delta(\omega)$  is still lacking,

because all published  $\delta(\omega)$  data have so far been obtained from  $T = 0$  up to  $T_0 < T_c$ , by consistently refraining from publishing  $\chi'(T \in [T_0, T_c])$ , whereas  $\chi''(T \in [T_0, T_c])$  data, albeit of little usefulness, are conversely *available* in the literature. This harmful state of affairs results from a long standing contradiction between the assumption  $\delta(\omega) = \lambda_L, \forall \omega$ , used in the interpretation of all experimental  $\delta(T < T_c)$ -data and the experimental evidence itself. It is thus in order to resolve this contradiction.

The expression of the average  $\delta$  in the two-fluid model has been shown [1] to read

$$\delta^{-2} = 2i\mu_0\omega \left( \frac{\sigma_n}{1 + i\omega\tau_n} + \frac{\sigma_s}{1 + i\omega\tau_s} \right). \quad (9)$$

As a consequence of the mainstream assumption [16]  $\tau_s \rightarrow \infty$ , Eqs. (1), (9) lead indeed to the complex impedance of the sample, reading as  $Z = \sigma_n(T) - i\omega\mu_0\lambda_L^2$ , and to  $\delta(\omega) = \lambda_L/\sqrt{2}, \forall \omega$ , respectively. Thence the average conductivity  $\sigma$ , equal to the real part of  $Z$ , is inferred to read, at low frequency such that  $\omega\tau_n \ll 1$ , as  $\sigma(T < T_c) = \sigma_n(T) = \frac{c_n(T)e^2\tau_n}{m} \Rightarrow \sigma(T < T_c) < \sigma_n(T_c) = \frac{c_0e^2\tau_n}{m}$ , because of  $c_0 > c_n(T < T_c) = c_0 - c_s(T)$ . As a matter of fact, both mainstream claims  $\delta(\omega) = \frac{\lambda_L}{\sqrt{2}}, \forall \omega$  and  $\sigma(T < T_c) < \sigma_n(T_c)$  are seen to run afoul at experimental evidence:

- the data, pictured in Fig. 3(a), show that  $\delta(\omega = 18 \text{ Hz}) \approx r_0 > 10^{-4} \text{ m}$ , whereas  $\lambda_L = \sqrt{\frac{m}{\mu_0 c_s e^2}} < 10^{-7} \text{ m}$ , so that  $\delta(\omega = 18 \text{ Hz}) \gg \lambda_L$ , which disproves the mainstream claim  $\delta(\omega) = \lambda_L, \forall \omega$ ;
- the measured, average ac conductivity for the superconducting phase of  $\text{YBa}_2\text{Cu}_3\text{O}_7$  has been reported [7, 8] to be  $\sigma(T < T_c) \approx 10^5 \sigma_n(T_c) \Rightarrow \sigma(T < T_c) \gg \sigma_n(T_c)$ , which rebuts the opposite claim  $\sigma(T < T_c) < \sigma_n(T_c)$ , inferred above from the mainstream view.

In summary, the only way to extract useful information from the  $\chi'$ -data, obtained at high frequency  $\omega \in [10 \text{ MHz}, 10 \text{ GHz}]$ , is to measure  $\chi'(T)$  up to  $T = T_c$  at two frequencies, distant from each other, as advised elsewhere [1].

## 5. CONCLUSION

The measured low-frequency susceptibility data in superconducting materials have been comprehensively explained within a recent account of the skin effect [1]. The prominent maximum of the absorption  $\chi''(T)$  has been associated with the steep decrease of the concentration of superconducting electrons  $c_s(T) \rightarrow 0$  for  $T \rightarrow T_c^-$  with the prerequisite  $|\delta(\omega, T_c)| > r_0$ , whereas the dispersion  $\chi'$  changing its sign at  $T_c$  has been identified to be the driving force of the Meissner effect, observed in a field-cooled sample [15].

Two remarks are of interest:

- by contrast with a normal metal, for which the temperature behavior of  $\sigma = \frac{c_0 e^2 \tau_n}{m}$  is completely determined by  $\tau_n(T)$ , as  $c_0$  remains constant,  $\sigma(T < T_c)$  in a superconductor is closely related to the variation of  $c_s(T)$ , because  $\tau_s$  is almost  $T$ -independent;
- the high frequency  $\delta$  assignments are obtained through the measurement of the dispersion  $\chi'$ , while the low frequency ones are obtained through that of the absorption  $\chi''$ .

Both assumptions  $\delta(\omega) = \lambda_L, \forall \omega$  and  $\lambda_L = \lambda_M$  have been rebutted. Therefore the determination of  $\delta$  paves the way for  $c_s(T < T_c)$  and the  $c_s$  dependence on the persistent current during the reversible superconducting-normal transition (see arXiv: 1704.03729). Accordingly, it is advised to carry out the  $\delta$ -measurement in the IR range [1], because the high frequency, such that  $\omega \tau_s \gg 1$ , ensures  $\delta(\omega) = \lambda_L / \sqrt{2}, \forall \omega$ , independent from  $\tau_s$ , which provides thereby direct access to  $c_s$ .

## ACKNOWLEDGMENT

We are indebted to Pr. A. Schilling for bringing to our attention two relevant publications [7, 8].

## REFERENCES

1. Szeftel, J., N. Sandeau, and A. Khater, "Study of the skin effect in superconducting materials," *Phys. Lett. A*, Vol. 381, 1525, 2017.
2. Maxwell, E. and M. Strongin, "Filamentary structure in superconductors," *Phys. Rev. Lett.*, Vol. 212, 10, 1963.
3. Strongin, M. and E. Maxwell, "Complex ac susceptibility of some superconducting alloys," *Phys. Lett.*, Vol. 49, 6, 1963.
4. Khoder, A. F., "The superconducting transition and the behavior of the ac susceptibility," *Phys. Lett. A*, Vol. 94, 378, 1983.
5. Bardeen, J., L. N. Cooper, and J. R. Schrieffer, "Theory of superconductivity," *Phys. Rev.*, Vol. 108, 1175, 1957.
6. Schrieffer, J. R., *Theory of Superconductivity*, Addison-Wesley, 1993.
7. Geshkenbein, V. B., et al., "ac absorption in the high- $T_c$  superconductors: Reinterpretation of the irreversibility line," *Phys. Rev. B*, Vol. 43, 3748, 1991.
8. Samarappuli, S., et al., "Comparative study of AC susceptibility and resistivity of a superconducting  $\text{YBa}_2\text{Cu}_3\text{O}_7$  single crystal in a magnetic field," *Physica C*, Vol. 201, 159, 1992.

9. Jackson, J. D., *Classical Electrodynamics*, John Wiley, 1998.
10. Born, M. and E. Wolf, *Principles of Optics*, Cambridge University Press, 1999.
11. Pippard, A. B., “The surface impedance of superconductors and normal metals at high frequencies,” *Proc. Roy. Soc. A*, Vol. 203, 98, 1950.
12. Hashimoto, K., et al., “Microwave penetration depth and quasiparticle conductivity of  $\text{PrFeAsO}_{1-y}$  single crystals: Evidence for a full-gap superconductor,” *Phys. Rev. Lett.*, Vol. 102, 017002, 2009.
13. Hashimoto, K., et al., “Microwave surface-impedance measurements of the magnetic penetration depth in single crystal  $\text{Ba}_{1-x}\text{K}_x\text{Fe}_2\text{As}_2$  superconductors: Evidence for a disorder-dependent superfluid density,” *Phys. Rev. Lett.*, Vol. 102, 207001, 2009.
14. London, F., *Superfluids*, Vol. 1, Wiley, 1950.
15. Szeftel, J., N. Sandeau, and A. Khater, “Comparative study of the Meissner and skin effects in superconductors,” *Progress In Electromagnetics Research M*, Vol. 69, 69–76, 2018.
16. Tinkham, M., *Introduction to Superconductivity*, Dover Books, 2004.
17. Ashcroft, N. W. and N. D. Mermin, *Solid State Physics*, Saunders College, 1976.